

MODELING OF TURBULENT SPRAY FLOWS USING AN IMPROVED MODEL FOR DROPLET MOTION

P. Wu and E. Gutheil

Interdisziplinäres Zentrum für Wissenschaftliches Rechnen

Ruprecht-Karls-Universität Heidelberg

Im Neuenheimer Feld 368, 69120 Heidelberg, Germany

Email: gutheil@iwr.uni-heidelberg.de, Phone: +49-6221-546114, Fax: +49-6221-546111

ABSTRACT

Turbulent spray flows usually involve large degrees of freedom and feature complex interactions between the turbulent gas flow and the spray. Therefore, a better understanding of turbulent two-phase flows is highly desirable. The objective of this paper is to improve the prediction of turbulent spray processes using a modified equation for droplet motion. In the current study, a stochastic term was added to the equation of droplet motion to account for the stochastic force. A comparison with experiments from the literature and with the results computed by the standard model shows better agreement for both the droplet velocity and Sauter mean radius. The fluctuations appearing in the profiles of droplet velocities and Sauter mean radius are considerably reduced, especially at axial locations near the injector. At axial locations far from the injector, the prediction of the Sauter mean radius near the centerline is improved.

Introduction

Turbulent spray flows are of enhanced interest in the frame of chemical, medical, pharmaceutical, and biological processes. In particular, the interaction of particles with the gas phase and the interaction with the turbulent flow are focus of many experimental and numerical investigations [1–3].

There is a number of numerical approaches that account for these processes. Even though sprays typically are dense in the area of spray injection and primary breakup and atomization, most studies apply Lagrangian – Eulerian approaches for the treatment of the gas and the spray since the alternative approach (Eulerian – Eulerian models) are still in their very initial stage of development. Within the first group of models, there are various popular approaches: They include direct numerical simulation (DNS) [4] as well as large eddy simulation (LES) [5], Reynolds averaged numerical simulations (RANS) and PDF (PDF – probability density function) [6]. The latter approach is used in the present paper where a joint gas velocity – mixture fraction PDF [7] is used to describe the gas phase as an improvement of the popular k - ϵ turbulence model.

In turbulent spray flows, there is a dominant effect of liquid phase processes on the entire spray flow and flame in case of reacting systems. This applies to both the liquid injection, atomization and evaporation processes. Even the dilute gas phase is strongly affected by the droplet and spray dynamics. Thus, the modeling and simulation of the liquid

phase is of special interest. The present paper focuses on the improved modeling of droplet motion.

Mathematical Model

The study concerns a two-dimensional axi-symmetric, steady and dilute spray flow. The present computations involve a non-reactive methanol spray flow. The model is an Eulerian–Lagrangian model for the gas and the spray, respectively.

Gas Phase

The gas phase equations comprise a one-point one-time Eulerian mass-weighted two-dimensional probability density function (PDF), \tilde{f} , [7]

$$\tilde{f}(\vec{V}, \zeta_C; \vec{x}, t) = \rho_g(\zeta_C) \langle \delta(\vec{U} - \vec{V}) \delta(\xi_C - \zeta_C) \rangle / \bar{\rho}_g \quad (1)$$

for the gas velocity and the mixture fraction where \vec{V} and ζ_C are the gas velocity and mixture fraction in sample space, resp., and \vec{U} and ξ_C are the corresponding variables in physical space. The transport equation of this PDF was derived following the work of [6] where extra source terms appear to account for interaction of the gas with the liquid phase. In particular, the evaporated mass, $\tilde{S}_{l,1}$ as well as the phase exchange source for momentum, \tilde{S}_{l,\vec{U}_i} , need to be considered. The resulting transported PDF equation yields [7]

$$\begin{aligned}
\bar{\rho}_g \frac{\partial \tilde{f}}{\partial t} &+ \bar{\rho}_g V_i \frac{\partial \tilde{f}}{\partial x_i} + \left(\bar{\rho}_g g_i - \frac{\partial \bar{p}}{\partial x_i} + \bar{S}_{l,\bar{v}_i} \right) \frac{\partial \tilde{f}}{\partial V_i} \\
&+ \frac{\partial (\bar{S}_{l,1} \tilde{f})}{\partial \zeta_C} \\
&= \frac{\partial}{\partial V_i} \left[\left\langle -\frac{\partial \tau_{ij}}{\partial x_j} + \frac{\partial p'}{\partial x_i} | \vec{V}, \zeta_C \right\rangle \tilde{f} \right] \\
&- \frac{\partial}{\partial \zeta_C} \left[\bar{\rho}_g \left\langle \frac{\partial}{\partial x_j} \left(D_M \frac{\partial \xi_C}{\partial x_j} \right) | \vec{V}, \zeta_C \right\rangle \tilde{f} \right].
\end{aligned} \tag{2}$$

In Eq. (2), τ_{ij} is the stress tensor in i - j -direction, D_M is the molecular diffusion coefficient of the mixture, and $\bar{\rho}_g$ is the mean gas density of the mixture. The terms on the left hand side appear in closed form, they include the terms of convection, body force, mean pressure gradient, and spray sources. The terms on the right hand side need to be modeled. They include the viscous stress tensor, the fluctuating pressure gradient, and the molecular diffusion flux. Due to the high dimensionality of the equation, a direct solution is not appropriate and a Lagrangian Monte-Carlo method is used to solve the equations. The flow is discretized into a large number of particles [8] where each particle has a set of properties $\{m_g^*, \vec{x}_g^*, \vec{U}_g^*, \xi_C^*\}$ where the superscript $*$ denotes the particle property. The PDF transport equation is transformed into a set of stochastic differential equations (SDE). The evolution of the gas particles in the velocity sample space is usually modeled using Langevin models [6, 12]. In the present paper, a simplified Langevin model is used which was extended to account for spray evaporation [7]:

$$\begin{aligned}
dU_i^*(t) &= \frac{1}{\bar{\rho}_g} \left(\bar{\rho}_g g_i - \frac{\partial \bar{p}}{\partial x_i} + \bar{S}_{l,\bar{v}_i} \right) dt \\
&- \left(\frac{1}{2} + \frac{3}{4} C_0 \right) \left(U_i^*(t) - \tilde{U}_i \right) \frac{\tilde{\epsilon}}{k} dt \\
&+ \sqrt{C_0 \tilde{\epsilon}} dW_i
\end{aligned} \tag{3}$$

The diffusion process is presented by a Wiener process $W(t)$ where $dW_i(t) = W_i(t+dt) - W_i(t)$ is Gaussian distributed with $\langle dW_i(t) \rangle = 0$ and $\langle dW_i(t) dW_j(t) \rangle = dt \delta_{ij}$. Effects of molecular diffusion are modeled using the IEM model [8] (IEM – interaction by exchange with the mean) which is also extended to account for spray evaporation:

$$\frac{d\xi_C^*(t)}{dt} = -\frac{1}{2} \frac{\tilde{\epsilon}}{k} C_\Phi \left[\xi_C^*(t) - \hat{\xi}_C \right] + \frac{\bar{S}_{l,1}}{\bar{\rho}_g} \tag{4}$$

The model constants are taken to be $C_0 = 2.1$ [12] and $C_\Phi = 2.0$ [8].

More details about the models and the solution methods may be found in Refs. [7–10].

The PDF transport equation is coupled with both the gas and the liquid phase equations. The conservation equations for the gas phase include the extended k - ϵ model [13], the continuity equation, and enthalpy. For a steady, two-dimensional, axi-symmetric turbulent liquid jet with no swirl, the Favre-averaged governing equations for the

particle-laden gas flow can be written as

$$\frac{\partial (\bar{\rho} \tilde{U}_i \tilde{\Phi})}{\partial x_i} - \frac{\partial}{\partial x_i} \left(\Gamma_{\phi,eff} \frac{\partial \tilde{\Phi}}{\partial x_i} \right) = \bar{S}_{g,\tilde{\Phi}} + \bar{S}_{l,\tilde{\Phi}} \tag{5}$$

where the boundary layer approximation was introduced. The conserved variables, $\tilde{\Phi}$, and the source terms for the gas, $\bar{S}_{l,\tilde{\Phi}}$, and the liquid phase, $\bar{S}_{g,\tilde{\Phi}}$, respectively, are presented in Ref. [13].

Liquid Phase

The liquid phase equations comprise droplet evaporation, heating, and motion.

Droplet Heating and Evaporation

For relatively small droplets with high volatility at atmospheric pressure, it is found [14, 15] that the distillation limit model, i.e. uniform droplet heating, performs well. In the present paper, the convective droplet heating and evaporation model of Abramzon and Sirignano [16]. The equations for droplet evaporation and heating yield:

$$\dot{m}_d = 2\pi \rho_F D_F r_d \hat{S} h \ln(1 + B_M) \tag{6}$$

and

$$m_d C_{p,l} \frac{dT_d}{dt} = \dot{m}_d \left(\frac{\hat{C}_{p,F}(T_{\infty,F} - T_d)}{B_T} - L_V(T_d) \right), \tag{7}$$

where m_d and \dot{m}_d are the droplet mass and evaporation rate, B_M and B_T the Spalding mass and heat transfer numbers, respectively. Indices F and d denote fuel and droplet parameters, respectively, and the superscript $\hat{}$ denotes averaged values in the film surrounding the droplet which are evaluated according to the 1/3 rule [17].

Droplet Motion

The equation for droplet velocities is modified to take into account the stochastic force on droplets exerted by the gas phase. The equation of droplet motion undergoing a random dispersion can be written in a similar way as the Langevin equation [19]:

$$\frac{dv_i}{dt} = \frac{3}{8} C_D \frac{\bar{\rho}}{\rho_L} \frac{|\tilde{u}_i - v_i|}{r} (\tilde{u}_i - v_i) + X, \tag{8}$$

where i is the index of the velocity vector components, C_D is the drag coefficient, \tilde{u}_i and $\bar{\rho}$ are the Favre averaged gas mean velocity and the mean density of the gas phase, respectively, ρ_L is the density of the liquid, r is the droplet radius, and X denotes the stochastic force which gives rise to the dispersion of the droplets in a turbulent flow, which is added in the present model. Equation (8) can be rewritten as

$$dv_i = (\tilde{u}_i - v_i) \frac{dt}{\tau_p} + X dt, \tag{9}$$

where

$$\tau_p = \left(\frac{3}{8} C_D \frac{\bar{\rho}}{\rho_L} \frac{|\tilde{u}_i - v_i|}{r} \right)^{-1} \tag{10}$$

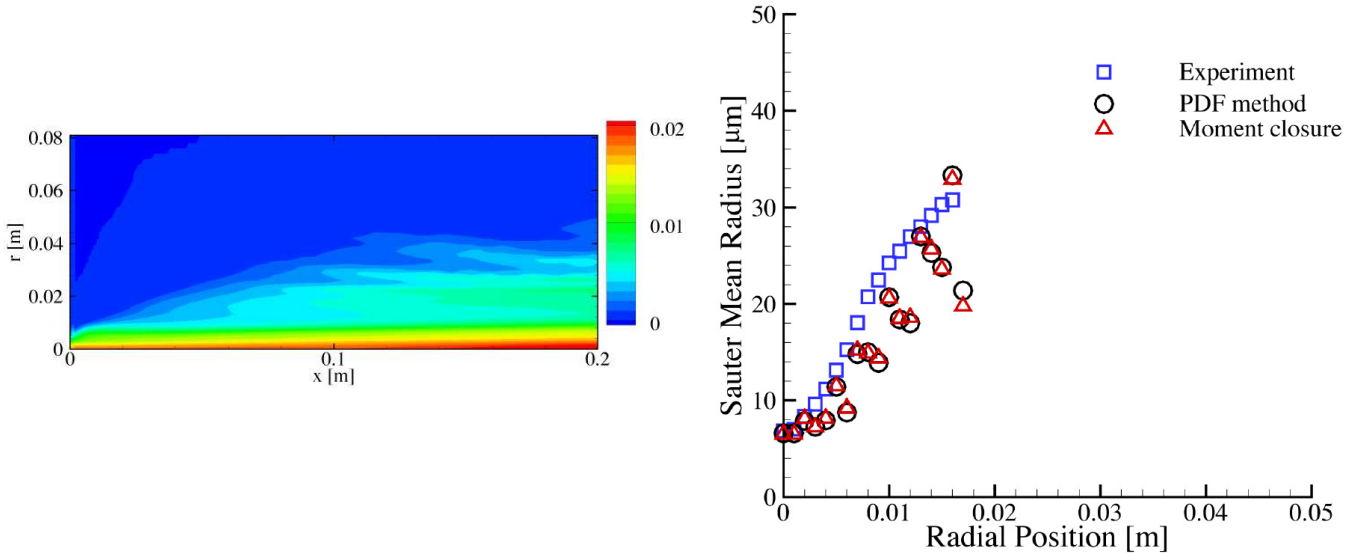


Figure 1: Contour plot of the methanol vapor mass fraction for the non-reacting methanol/air spray flow (left) and radial profile of the Sauter mean Radius of the spray at $x = 25$ mm (right) [7, 21]

is the droplet response time. The stochastic force, X , then is given as [19]:

$$X = \xi \sqrt{C_0 \tilde{k} / \tau_p} dt, \quad (11)$$

where ξ is a dimensionless quantity following a standard normal distribution, \tilde{k} is the gas phase Favre-averaged turbulent kinetic energy. Jones and Sheen [19] determined the empirical constant, C_0 , to attain the value 1.0. In the present computations, values from 0.5 to 5.0 are tested. It turns out that the results with $C_0 = 2.0$ give the best prediction for the droplet properties for the experiment studied here.

Numerical Solution

The numerical solution procedure involves a hybrid method for the gas and the liquid phase equations. The liquid phase is solved in Lagrangian coordinates where a special numerical procedure is used to solve for the droplet motion. Details are given in Ref. [18].

The finite-volume equations, c.f. Eqs. (5), are solved using a SIMPLE based algorithm where special care is to be taken for the implementation of source terms [13, 20].

The PDF transport equation is solved using a Monte-Carlo method which is extensively discussed in Refs. [9, 10].

Results and Discussion

The modified equation for droplet motion has been implemented into an existing Eulerian-Lagrangian code [7–10], the first two of which are used to simulate turbulent non-reactive methanol/air spray flows. The experiments taken for comparison with the simulation were conducted by McDonell and Samuelsen [21].

The experiments by McDonell and Samuelsen have been extensively used for comparison with various models such as the RANS model with extended $k-\epsilon$ model [13, 20] as well as the Reynolds stress model for spray flows [11] and

the joint PDF transport equation for both non-reacting [7, 8] and reacting sprays [9] so that a wide data base is available.

The paper presents a comparison of results using the standard equation of droplet motion and the equation using the term describing the stochastic force, c.f. Eq. 8. For comparison of the influence of this term, a comparison of the PDF method with the RANS model (extended $k-\epsilon$ model) is given.

The left part of Fig. 1 shows the contour plot of the methanol vapor mass fraction. It is found that major methanol vapor is found near the axis of the flow field where major evaporation occurs.

The right part of Fig. 1 displays a radial profile of the Sauter mean radius of the spray at $x = 25$ mm from the nozzle. It can be seen that the methods do not differ too much, and the values fluctuate. Overall, the experimental values are underpredicted by the numerical computations. This may have several reasons. First, the numerical particle technique involves a procedure to keep the particle number in a cell within a certain range. This procedure currently involves discard of the smallest particles which may lead to a mass loss. This issue needs to be addressed in a future study. Moreover, the experiments discard droplets which appear non-spherical. If these droplets are smaller than the Sauter mean radius, this procedure may lead to an overprediction of Sauter mean radius. The main point to be learnt from the RHS of Fig. 1 is that the RANS and the PDF model do not lead to very different results for the Sauter mean radius. This is attributable to the fact that the major differences between the models appear in the gas phase characteristics, and therefore, minor effect is to be expected in the liquid phase. The second point both models show is that the fluctuation of the Sauter mean radius is present in both models in contrast to the experimental data.

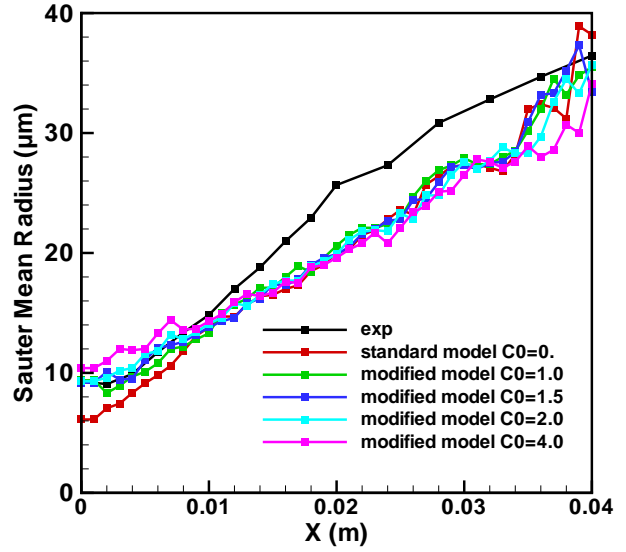
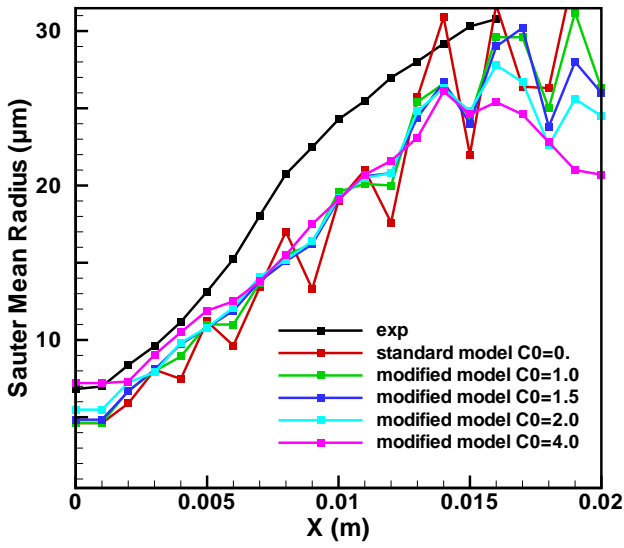


Figure 2: Radial profiles of the Sauter mean radius (SMR) with different values for C_0 at $x = 25$ mm (left) and 100 mm (right)

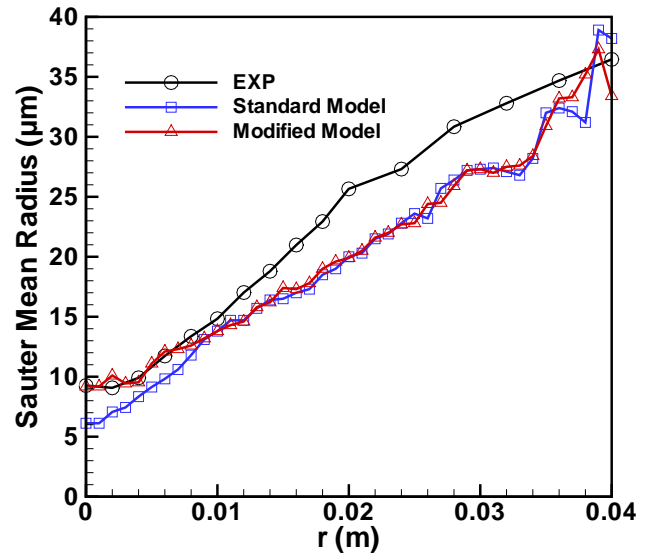
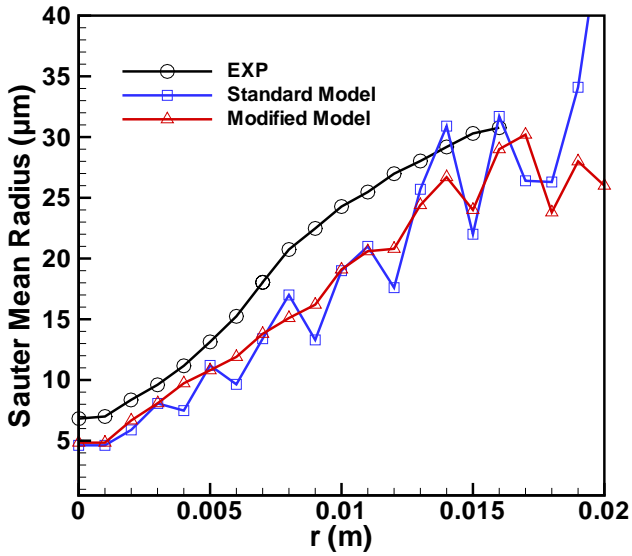


Figure 3: Radial profiles of the Sauter mean radius at $x = 25$ mm (left) and 100 mm (right)

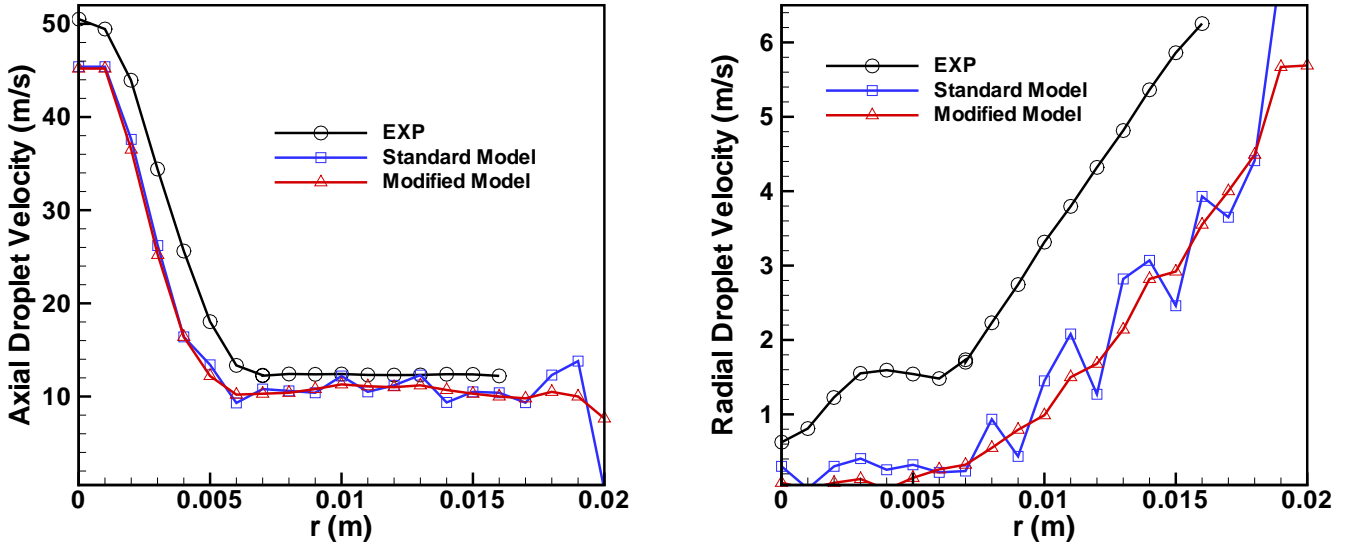


Figure 4: Radial profiles of the axial velocity(left) and radial velocity(right) of the droplet at $x = 25$ mm

Figure 2 shows a comparison of the Sauter mean radius for experimental data and numerical simulations with different constants, C_0 , see Eq. (11). Two radial profiles at $x = 25$ mm (left) and $x = 100$ mm (right) are displayed. Symbols denote positions where spray exists, and they are connected even though the distribution is discrete for improved visibility. The left-hand side of Fig. 2 shows that at $x = 25$ mm from the inlet, the experimental results are rather smooth whereas the numerical results anticipate considerable fluctuations. The value of C_0 is varied between zero and five where zero represents the standard model with discarded term for statistical force, c.f. Eq. (11). These fluctuations decrease with increasing value of C_0 . At the same time, the values on the axis of symmetry decrease with increasing the value of the constant C_0 and at the outer spray boundary, this observation is reversed. It seems that an intermediate value of 2 is a good compromise between these effects caused by the variation of C_0 .

The right hand side of Fig. 2 shows radial profiles of the Sauter mean radius at 100 mm distance from the spray inlet. Here, all profiles appear to be much smoother independent of the value of the constant C_0 at least in the intermediate droplet size range. For small values of the Sauter mean radius near the axis of symmetry, an increased value of C_0 increases the values of the Sauter mean radii whereas the effect is reversed at the high values of Sauter mean radius at the boundary of the spray jet.

Figure 3 shows radial profiles of the Sauter mean radius at the same positions where a comparison between the standard model and the modified model with $C_0 = 2$ for the same axial locations shown in Fig. 2. The left-hand side of Fig. 3 may be compared to the right part of Fig. 1 to see the influence of the different models used. It can be seen that the consideration of the stochastic force leads to smoother profiles compared to the models where this term is neglected. Moreover, the range of differences between the

PDF, the standard model, and the model including the term of stochastic force are about in the same range. The differences between the moment closure or RANS method and the PDF method are minor because the PDF was applied for gas-phase variables and therefore, they only indirectly affect the spray. The stochastic force should be included to yield a smoother profile of the Sauter mean radius and avoid artificial fluctuations.

All models underpredict the experimental values of the Sauter mean radius. This may be attributable to various reasons. The experimental data are coarse and therefore, there is some ambiguity in defining the initial values of the liquid phase characteristics such as droplet size and velocity which greatly affects to numerical computations. An underprediction may result. Moreover, the PIV measurements discard droplets which are not spherically symmetric and therefore, an overprediction of the Sauter mean radius occurs if smaller droplets are neglected. The numerical model also may lead to an underprediction because of negligence of droplet collisions and interaction between droplets such as effects of evaporation in presence of droplets which may lead to additional insecurities.

A comparison of the profiles at $x = 25$ mm and 100 mm shows that the profiles further away from the fuel inlet show less effect by the term accounting for stochastic force. The right-hand side of Fig. 4 shows that the profiles are almost identical except for near the centerline where the standard model underpredicts the Sauter mean radius.

Conclusions

The equation for droplet motion has been extended by a term to account for the influence of the stochastic force. Radial profiles of droplet size and velocities were compared using the standard model and the model including the stochastic force at two different axial locations. The results of the standard model have remarkable fluctuations at the axial

position $x = 25$ mm, while the results of the modified model are much smoother. The poor performance of the standard model is mainly due to its insufficiency of capturing the stochastic interaction between the droplets and the turbulent gas flow. At the axial position $x = 100$ mm, the results of the Sauter mean radius predicted by the modified model of droplet motion improve the prediction compared to experiment near the centerline, while fail to give better prediction off the centerline. Nevertheless, the modified model fails to alter the average level of the droplet size and velocities.

Acknowledgement

Financial support from German Science Foundation (DFG) through International Graduate College 710 is gratefully acknowledged.

References

- [1] J. J. Granier, M. L. Pantoya: *The Effect of Size Distribution on Burn Rate in Nanocomposite Thermite: A Probability Density Function Study*, *Combust. Theory Modelling* **8** (2004) 555-565.
- [2] P. S. Karasso, M. G. Mungal: *Mixing and reaction in curved liquid shear layers*, *J. Fluid Mech.* (1997), Vol. 334, 381-409.
- [3] A. N. Karpetis, A. Gomez: *An Experimental Study of Well-Defined Turbulent Nonpremixed Spray Flames*, *Combust. Flame* **121**: 1-23 (2000).
- [4] T. Baritaud: *Direct Numerical Simulation for Turbulent Reactive Flows*, Editions Technip, 1996.
- [5] B. Geurts: *Elements of Direct and Large Eddy Simulation*, R. T. Edwards Inc., 2003.
- [6] S. B. Pope: *PDF methods for turbulent reactive flows*. *Prog. Energy Combust. Sci.*, **11**:119-192 (1985).
- [7] H.-W. Ge, E. Gutheil: *Joint Velocity-Scalar PDF Modeling of Turbulent Spray Flows*, 20th ILASS Europe Conference, Orléans, France, Sept. 5.-7, 2005.
- [8] H.-W. Ge, E. Gutheil: *PDF Simulation of Turbulent Spray Flows*. *Atomization and Sprays*, Vol.16(5), 531-542 (2006).
- [9] H.-W. Ge, E. Gutheil: *Simulation of a Turbulent Spray Flame Using Coupled PDF Gas Phase and Spray Flamelet Modeling*, *Combustion and Flame*, Vol. 153/1-2 pp 173-185, 2008. DOI:10.1016/j.combustflame.2007.10.019.
- [10] H.-W. Ge, I. Dwel, H. Kronemayer, R. W. Dibble, E. Gutheil, C. Schulz, J. Wolfrum: *Laser based experimental and Monte Carlo PDF numerical investigation of an ethanol/air spray flame*, *Combustion Science and Technology* **180**: 1529-1547, 2008.
- [11] H.-E. Ge, D. Urzica, M. Vogelgesang, E. Gutheil, *Modeling and Simulation of Turbulent Non-Reacting and Reacting Spray Flows*. in: *Reactive Flows, Diffusion and Transport* (W. Jäger, R. Rannacher, J. Warnatz, Eds.), Springer 2007.
- [12] D. C. Haworth, S. B. Pope: *A generalized Langevin model for turbulent flows*. *Phys. Fluids*, **29**:387-405(1986).
- [13] C. Hollmann, E. Gutheil: *Modeling of Turbulent Spray Diffusion Flames Including Detailed Chemistry*, *Proc. Combust. Inst.* **26**, Vol. 1, 1731-1738 (1996).
- [14] C. K. Law: *Recent Advances in Droplet Vaporization and Combustion*, *Prog. Energy Combust. Sci.*, **8**, 171-201, 1982.
- [15] W. A. Sirignano: *Fluid Dynamics and Transport of Droplets and Sprays*. Cambridge University Press (1999).
- [16] B. Abramzon, W. A. Sirignano: *Droplet vaporization model for spray combustion calculation*. *Int. J. Heat Mass Transfer*, **9**:1605-1618(1989).
- [17] G. L. Hubbard, V. E. Denny, A. F. Mills: *Droplet Evaporation: effects of transients and variable properties*. *Int. J. Heat Mass Transfer*, **18** (9):1003-1008(1975).
- [18] H.-W. Ge, E. Gutheil: *An Efficient Numerical Solution Scheme for the Computation of the Particle Velocity in Two-Phase Flows*, *Progress in Computational Fluid Dynamics*, Vol. 7 (8), 467-472, 2007.
- [19] W. P. Jones, D.-H. Sheen: *A probability density function method for modelling liquid fuel sprays*, *Flow, Turbulence and Combustion* **63**, 379 (1999)
- [20] C. Hollmann, E. Gutheil: *Flamelet modeling of turbulent spray diffusion flames based on a laminar spray flame library*, *Combustion Science and Technology* **135**, 175 (1998)
- [21] V. G. McDonell, G. S. Samuelsen: *An experimental data base for computational fluid dynamics of reacting and nonreacting methanol sprays*, *J. Fluids Engin.* **117**, 145 (1995)